HHS Public Access

Author manuscript

Oncogene. Author manuscript; available in PMC 2015 January 10.

Published in final edited form as:

Oncogene. 2014 July 10; 33(28): 3660–3667. doi:10.1038/onc.2013.342.

Activation of Akt Signaling in Prostate Induces a TGFβ Mediated Restraint on Cancer Progression and Metastasis

Glen A. Bjerke[1], **Chun-Song Yang**[1], **Henry F. Frierson**[2], **Bryce M. Paschal**[1], and **David Wotton**[1,#]

[1] Department of Biochemistry and Molecular Genetics, and Center for Cell Signaling, University of Virginia, Charlottesville, USA

[2] Department of Pathology, University of Virginia, Charlottesville, USA

Abstract

Mutations in the *PTEN* tumor suppressor gene are found in a high proportion of human prostate cancers, and in mice, *Pten* deletion induces high-grade prostate intra-epithelial neoplasia (HGPIN). However, progression from HGPIN to invasive cancer occurs slowly, suggesting that tumorigenesis is subject to restraint. We show that *Pten* deletion, or constitutive activation of the downstream kinase AKT, activates the transforming growth factor (TGF) β pathway in prostate epithelial cells. TGFβ signaling is known to play a tumor suppressive role in many cancer types, and reduced expression of TGFβ receptors correlates with advanced human prostate cancer. We demonstrate that in combination either with loss of *Pten*, or expression of constitutively active AKT1, inactivation of TGFβ signaling by deletion of the *TGFβ type II receptor* gene relieves a restraint on tumorigenesis. This results in rapid progession to lethal prostate cancer, including metastasis to lymph node and lung. In prostate epithelium, inactivation of TGFβ signaling alone is insufficient to initiate tumorigenesis, but greatly accelerates cancer progression. The activation of TGFβ signaling by Pten loss or AKT activation suggests that the same signaling events that play key roles in tumor initiation also induce the activity of a pathway that restrains disease progression.

Keywords

TGFβ; Akt; Pten; prostate cancer; signaling

Introduction

Deletions or mutations in *PTEN* are found in 30% of primary human prostate cancers, and more than 60% of prostate cancer metastases [1-4]. A major consequence of PTEN loss is

[#]Corresponding author: David Wotton Center for Cell Signaling, University of Virginia, Box 800577, HSC, Charlottesville VA 22908 dw2p@virginia.edu voice: 434-243-6752 fax: 434-924-1236.

Conflict of Interest

The authors declare no conflict of interest.

deregulated PI3-kinase signaling leading to activation of Akt/PKB, an oncogenic kinase that promotes cell growth, proliferation and survival [5, 6]. Although homozygous deletion of *Pten* in mice is embryonic lethal, animals with heterozygous loss of function develop tumors in multiple tissues, including the prostate [7, 8]. Conditional deletion of *Pten* in mouse prostate activates Akt signaling and causes focal prostate intraepithelial neoplasia (PIN) by 6 weeks and high grade PIN (HGPIN) by 8-9 weeks. These mice develop locally invasive tumors by 6-12 months but usually survive beyond one year of age [9-12]. Homozygous deletion of *Akt1* slows the development of HGPIN in *Pten* heterozygous mice, and reducing levels of PDK1, which is required for activation of Akt, also slows tumor formation in *Pten* heterozygotes [13, 14]. Akt signaling is, therefore, a major mediator of the tumorigenic effects of Pten loss. A transgenic line in which constitutively active human AKT1 (caAKT1) is expressed from the rat probasin promoter develops HGPIN with high penetrance, but these tumors do not become invasive [15, 16]. Thus, while Akt is a key driver of the HGPIN phenotype induced by loss of Pten, additional factors are required for progression to invasive cancer. In addition, while homozygous loss of *Pten* efficiently initiates prostate tumorigenesis, tumors in these mice progress beyond HGPIN relatively slowly, suggesting the presence of pathways that limit tumor progression.

Transforming growth factor (TGF) β ligands assemble a complex of type I and type II receptors, in which the type II receptor phosphorylates and activates the type I receptor [17-19]. The activated type I receptor phosphorylates receptor Smads (R-Smad), primarily Smad2 and Smad3 in response to TGFβ, and phosphorylated R-Smad/Smad4 complexes accumulate in the nucleus to regulate gene expression [20]. In many cell types, including epithelial cells, TGFβ signaling via Smad2/3 inhibits cell proliferation and plays a tumor suppressive role [21, 22]. Mutations in the *TGFβ type I* and *type II receptor* (*TGFBR1* and *2*) genes are observed in human prostate cancer [23], and reduced expression of *SMAD4* and *TGFBR2* correlates with advanced prostate cancer [24, 25]. A reduction in expression of TGFBR1 and TGFBR2, has been reported in up to 25% and 12.5%, respectively, of human prostate cancers, and reduced TGFBR2 expression was also shown to correlate with decreased survival [23, 26-28]. In mice, the combination of prostate-specific homozygous *Pten* deletion with homozygous mutations in *Smad4*, which encodes a mediator of TGFβ family signaling, has been shown to drive aggressive prostate tumors [29]. Together with elevated Cyclin D and Spp1 expression, reduced expression of Pten and Smad4 was suggested be predictive of human prostate cancer severity. Additionally, in a mouse prostate cancer model with telomere dysfunction and genomic instability, deletion of the *Smad4* gene was seen in a significant proportion of tumors [30]. Thus TGFβ signaling is likely a key regulator of prostate cancer progression.

Here we show that deletion of *Pten* or expression of constitutively active AKT1 in the prostate results in induction of multiple components of the TGFβ pathway. Homozygous deletion of *Tgfbr2* specifically in prostate epithelial cells in the background of a *Pten* mutation results in the rapid onset of poorly differentiated adenocarcinoma of the prostate that is refractory to castration. Micro-invasive cancer is evident as early as 8 weeks after birth, and animals lacking both Pten and Tgfbr2 from the prostate develop lymph node and lung metastases. Finally, we provide evidence that the combination of constitutive Akt

activation together with inactivation of TGFβ signaling is sufficient to generate invasive cancer in the prostate.

Results

Early onset of lethal prostate cancer in the absence of both *Pten* and *Tgfbr2*

To test whether deletion of the *Tgfbr2* gene affected prostate cancer progression in mice we combined conditional alleles of the *Tgfbr2* [31] and *Pten* genes [10] with the prostate epithelium-specific CRE transgene (*Pb-Cre4*; [32]). Analysis of mouse prostate tissue by IHC revealed relatively low level expression of Tgfbr2 in prostate epithelium, that was lost with the conditional *Tgfbr2* allele and the *Pb-Cre4* transgene (Figure 1A). To confirm the effects of loss of *Pten*, we stained wild type and conditional *Pten* null prostate with an antibody that recognizes Akt phosphorylated on serine 473, as a mark of Akt activation. Little or no phospho-Akt signal was seen in the control, whereas Akt activation was clearly present in the conditional *Pten* null prostate (Figure 1A). We next generated males with homozygous deletion of both genes in the prostate (referred to as $Pten^{r/r};Tgfbr2^{r/r}$). From 32 $Pten^{r/r};Tgfbr2^{r/r}$ male mice, none survived past 20 weeks of age, median survival time was less than 13 weeks (88 days), and five animals required euthanasia prior to 11 weeks of age (Figure 1B and E). In contrast, no *Pten* or *Tgfbr2* single null animals showed excessive tumor burden during this time-course, and $Tgfbr2^{r/r}$ males survived to 70 weeks without any apparent phenotype. Examination of $Pten^{r/r};Tgfbr2^{r/r}$ animals that required euthanasia revealed the presence of dense prostate tumors with bladder obstruction (Figure 1C), which appeared to arise primarily from the ventral prostate, although all lobes were affected in most animals.

Tumor progression was also analyzed in 36 *Pten* heterozygotes with different *Tgfbr2* genotypes. All 17 animals that were wild type or heterozygous for *Tgfbr2* survived to 70 weeks, whereas most $Pten^{+/r};Tgfbr2^{r/r}$ mice had to be euthanized prior to 70 weeks of age (Figure 1D). Compared to $Pten^{+/r}$ or $Pten^{+/r};Tgfbr^{+/r}$ mice there was a significant increase in the incidence of invasive cancer in the $Pten^{+/r};Tgfbr2^{r/r}$ mice, with a concomitant decrease in median survival to less than 49 weeks (Figure 1D). $Pten^{+/r};Tgfbr2^{r/r}$ mice developed large prostate tumors similar to those seen in double nulls (Figure 1C and E). The effect of homozygous *Tgfbr2* deletion on the survival of *Pten* null and *Pten* heterozygous animals was highly significant, demonstrating a dramatic synergistic effect of deleting both *Tgfbr2* and *Pten* in the prostate (Figure 1B and D). Additionally, even a heterozygous mutation in the *Tgfbr2* gene resulted in more rapid onset of severe tumors in a *Pten* null background, reducing the median survival time by almost 6 months (Figure 1E).

Invasive adenocarcinoma in $Pten^{r/r};Tgfbr2^{r/r}$ prostates

Histological analysis of prostates from $Tgfbr2^{r/r}$ mice did not reveal any differences compared to wild type animals, even beyond one year of age (Figure 2A and data not shown). By 8 weeks of age both $Pten^{r/r}$ and $Pten^{r/r};Tgfbr2^{r/r}$ animals had developed HGPIN with 100% penetrance (Figure 2). Regions of micro-invasive cancer were evident in the majority of $Pten^{r/r};Tgfbr2^{r/r}$ prostates as early as 8 weeks of age, and by 12-14 weeks this had progressed to poorly differentiated adenocarcinoma (PDA), although regions of HGPIN

were also visible in many samples (Figure 2). In contrast, breakdown of the ductal structure of the prostate was minimal in *Pten* null animals with HGPIN being the predominant phenotype to at least 25-30 weeks of age.

To test whether proliferation was different in *Pten*$^{r/r}$;*Tgfbr2*$^{r/r}$ compared to *Pten*$^{r/r}$ prostates, we stained sections with antibodies against Ki-67 and Cyclin D, which has been shown to be increased in highly proliferative prostate cancer [29]. Quantitative analysis of the four genotypes, with areas of HGPIN and PDA counted separately in the *Pten*$^{r/r}$;*Tgfbr2*$^{r/r}$ animals, revealed no significant difference between wild type and *Tgfbr2* null prostates. In contrast, HGPIN in either *Pten*$^{r/r}$ or *Pten*$^{r/r}$;*Tgfbr2*$^{r/r}$ animals had significantly higher numbers of Cyclin D positive cells (Figure 3A and B). Similar analyses for the proliferation marker, Ki-67, revealed increased staining in HGPIN compared to normal tissue (Figure 3C). Comparison of PDA to HGPIN in *Pten*$^{r/r}$;*Tgfbr2*$^{r/r}$ animals showed a significant increase in both Cyclin D and Ki-67 staining, whereas no differences between *Pten*$^{r/r}$ and *Pten*$^{r/r}$;*Tgfbr2*$^{r/r}$ HGPIN were observed (Figure 3B and C). Examination of expression of the CDK inhibitor, p27 (Cdkn1b), revealed an increase in the number of positive cells in the *Pten*$^{r/r}$, that was reversed in the double mutant samples (Figure 3D). Changes in nuclear Cyclin D and p27 expression correlated with phenotype in *Pten*$^{r/r}$ and *Pten*$^{r/r}$;*Tgfbr2*$^{r/r}$ animals, with higher Cyclin D levels in invasive cancer than adjacent HGPIN or normal ducts, and the converse for p27 (Figure 3E). Thus increased proliferation appears to correlate with phenotype as the tumors progress from HGPIN to invasive cancer in the double null animals.

Castration-resistant metastasis in the double null animals

We examined the lumbar lymph nodes for metastases from 50 *Pten*$^{r/r}$ mice with different *Tgfbr2* genotypes. Only one of six *Pten* null mice had a lymph node micro-metastasis, whereas 23 out of 35 *Pten*$^{r/r}$;*Tgfbr2*$^{r/r}$ mice had lymph node metastases, as well as all nine of the *Pten*$^{r/r}$;*Tgfbr2*$^{+/r}$ mice examined (Figure 4A). In addition, four of the eleven *Pten*$^{+/r}$;*Tgfbr2*$^{r/r}$ animals examined had lymph node metastases, most of which were relatively small, but could be readily confirmed by staining for keratin 18 (Figure 4B and C). Lymph node metastases were found in a high proportion of *Pten* mutant animals that also had mutations in *Tgfbr2*, suggesting that impaired TGFβ signaling in the context of a *Pten* mutation can promote invasion and metastasis. We also examined other tissues in a subset of mice that were positive for lymph node metastasis. Lung metastases were found in all four *Pten*$^{r/r}$;*Tgfbr2*$^{+/r}$ mice examined, and at a lower frequency (6 out of 11) in *Pten*$^{r/r}$;*Tgfbr2*$^{r/r}$ mice (Figure 4D). As with lymph node, the majority of lung metastases were very small, although one much larger metastasis was found in a *Pten*$^{r/r}$;*Tgfbr2*$^{+/r}$ mouse (Figure 4E and F).

Androgen ablation is a common treatment for human prostate cancer that is initially effective at reducing tumor growth [33]. To test whether tumor progression in *Pten*$^{r/r}$;*Tgfbr2*$^{r/r}$ mice would respond to castration, we castrated 8 animals at 6 weeks, prior to the onset of adenocarcinoma, and eight at 9-11 weeks of age when the tumors are more advanced. Mice castrated either at 6 weeks, or after 9 weeks of age had a median survival time of 93 and 95 days, compared to 88 days for the intact animals. Even when combining the data for all

castrated animals, there was only a slight rightward shift in the survival curve, which was not significant (Figure 4G). We also identified lymph node micro-metastases in 5 of 14 castrated animals examined (Figure 4A). While this is less frequent than in the intact animals, the difference does not reach significance with this number of animals. These data suggest that tumor initiation and progression to invasive metastatic disease in *Pten*$^{r/r}$;*Tgfbr2*$^{r/r}$ prostates is insensitive to depletion of testicular androgens.

Induction of TGFβ signaling by Pten loss

IHC analysis of Tgfbr2 and Smad4 revealed that expression of both proteins was increased, specifically in epithelial cells in *Pten*$^{r/r}$ prostates (Figure 5A). By qRT-PCR, expression of both *Tgfbr2* and *Smad4*, as well as *Tgfb1* and *Smad3* was increased in the *Pten*$^{r/r}$, and smaller increases in *Smad2* and *Tgfbr1* were observed (Figure 5B). The increases in Tgfbr2 and Smad4 expression were confirmed at the protein level by western blot (Figure 5C). To verify that increased expression of TGFβ pathway components results in pathway activation, we examined expression of Smad2 phosphorylated at the carboxyl-terminal receptor phosphorylation site (pSmad2). A clear increase in active pSmad2 was evident in the *Pten* null (Figure 5C). To determine whether TGFβ signaling to Smad2 changed specifically in epithelial cells, we examined levels of pSmad2 by immunofluorescence microscopy (Figure 5D). Comparison of the mean nuclear to cytoplasmic (N:C) ratio for pSmad2 did not reveal a change between the control and *Tgfbr2* null, consistent with low levels of TGFβ receptor expression and minimal pathway activity in the wild type controls (Figure 5E). However, there was a significant increase in the N:C ratio in *Pten*$^{r/r}$ compared to wild type, suggesting that the increase in pathway components results in increased nuclear phospho-Smad2 in *Pten*$^{r/r}$ prostate epithelium. Comparison of *Pten*$^{r/r}$;*Tgfbr2*$^{r/r}$ with *Pten*$^{r/r}$ prostate showed a significant decrease in the pSmad2 N:C ratio, consistent with the loss of Tgfbr2 (Figure 5E). It should be noted that the pSmad2 level was still higher in the double null than in the wild type, suggesting that signaling via activin type II receptors may drive some Smad2 phosphorylation in the absence of Tgfbr2. Together these data suggest that Pten loss induces up-regulation of the TGFβ pathway.

Akt activates TGFβ signaling

Transgenic expression of a myristoylated AKT1 in the prostate (*Tg-AKT*) results in constitutive AKT1 activity in epithelial cells, and the majority of these mice develop HGPIN, primarily in the ventral prostate [16]. Since Akt activation is one of the major outcomes of Pten loss, we tested whether *Tg-AKT* could induce TGFβ pathway activity. High levels of Smad4 expression were evident in *Tg-AKT* prostate, whereas expression was much lower in the control (Figure 6A). Increased expression of Smad4 was observed in regions of the *AKT1* transgenic prostate in which pAkt was detectable, and in which the HGPIN phenotype was evident, but not in pAkt negative samples, in which no phenotype was apparent (Figure 6A). Analysis of Tgfbr2 and Smad4 by western blot revealed an increase in expression in the AKT transgenic prostate, as well as an increase in pSmad2 levels (Figure 6B). To test for increased TGFβ pathway activity we analyzed the pSmad2 N:C ratio in two pAkt positive *AKT1* transgenics, as well as a *Pten*$^{r/r}$ sample for comparison. We observed significant increases in the pSmad2 N:C ratio in both *Tg-AKT*

samples compared to wild type (Figure 6C). Taken together, these data suggest that TGFβ pathway activation in response to loss of *Pten* occurs downstream of Akt activation.

We next tested whether prostate cancer progression in the *Tg-AKT* model is limited by TGFβ signaling. Unlike the *Pten* null model, HGPIN in *Tg-AKT* mice does not progress to invasive cancer in the absence of other targeted mutations [16, 34]. We monitored a group of 17 *Tg-AKT* mice to 70 weeks of age, of which nine were homozygous null for *Tgfbr2*. Four of the nine *Tgfbr2*$^{r/r}$ were euthanized before 70 weeks of age due to tumor burden, whereas all eight mice that were wild type for the receptor survived (Figure 6D). We found invasive cancer in several *Tg-AKT;Tgfbr2*$^{r/r}$ mice, whereas, this was not observed in *Tg-AKT* mice that were wild type for *Tgfbr2*. HGPIN with high levels of nuclear cyclin D staining was observed in *Tg-AKT* and *Tg-AKT;Tgfbr2*$^{r/r}$ prostates. However, cyclin D staining was further elevated in regions of invasive cancer, in the ventral prostate of *Tg-AKT;Tgfbr2*$^{r/r}$ mice, consistent with increased proliferation in these animals (Figure 6E). More than 80% of *Tg-AKT* and *Tg-AKT;Tgfbr2*$^{r/r}$ animals had HGPIN after 10 weeks of age (Figure 6F). However, 5 out of 15 of the phenotypic *Tg-AKT;Tgfbr2*$^{r/r}$ animals also had invasive cancer, and this increased to 4 out of 9 among the older animals (Figure 6F). Together, these data suggest that Akt activation triggers a TGFβ-mediated tumor restraint mechanism in prostate epithelium, and that inactivation of this restraint accelerates tumor progression.

Discussion

We found that loss of both Pten and the Tgfbr2 from mouse prostate results in aggressive, castration resistant cancer with lymph node and lung metastases. Thus loss of both Pten and Tgfbr2 from mouse prostate appears to recapitulate several features of advanced human prostate cancer, including resistance to androgen depletion and metastasis to distant organs. The most surprising result from our analysis of *Tgfbr2;Pten* mutants, and from previous work with *Smad4;Pten* mutants [30], is that loss of Pten causes up-regulation of multiple components of the TGFβ pathway, a signaling pathway that restrains tumor progression. Importantly, we show that there is an increase in activated nuclear Smad2 specifically in epithelial cells in *Pten* null tumors. Additionally, we showed that expression of a constitutively active *AKT1* transgene that induces HGPIN [16], is sufficient to induce Smad4 expression and increase the level of nuclear phospho-Smad2. This suggests that TGFβ pathway activation causes by loss of Pten occurs downstream of Akt, rather than other pathways that may be activated by *Pten* deletion. It is possible that this Akt-mediated activation of the TGFβ pathway occurs in response to the HGPIN phenotype, rather than as a direct result of Akt activation. However, since more than one component of the TGFβ pathway is up-regulated by Pten loss, multiple mechanisms may be responsible for the increased expression. Given that prostate cancer can remain indolent for years, it will be of interest to know whether other mutations linked to prostate cancer also activate the TGFβ mediated restraint, and whether an inactivating mutation in the TGFβ pathway can promote tumor progression in conjunction with defects in pathways other than the Pten/Akt pathway.

Expression of caAKT1 in mouse prostate induces HGPIN, but these tumors do not progress to invasive cancer [16, 34]. In contrast, in *Pten* null prostate HGPIN progresses to invasive cancer, albeit much more slowly than in the presence of an inactivating mutation in the

TGFβ pathway. Although the TGFβ-mediated restraint is activated by caAKT1, and we show that *Tgfbr2* deletion is sufficient to allow progression of *Tg-AKT* tumors to invasive cancer, this still occurs much more slowly than in the *Pten* null model. Deletion of *Cdkn1b* in the context of a heterozygous *Pten* mutation accelerates tumorigenesis in prostate and other tissues [35]. Similarly, the combination of prostate-specific *Tg-AKT* with a constitutive *Cdkn1b* deletion results in a proportion of tumors becoming invasive, although in most cases this occurred only after one year of age [34]. We found that homozygous deletion of *Tgfbr2* in the context of both prostate epithelium-specific *Pten* deletion and of *Tg-AKT* tumors results in progression to invasive cancer, but still with a very different time-course. Thus it is likely that, in addition to Akt activation, other pathways activated in response to Pten loss help drive progression to invasive cancer. However, an alternative explanation for this difference is that the expression of myristoylated AKT1 in the prostate is unable to fully recapitulate the effects of AKT activation resulting from Pten deletion.

Our analysis of mice with prostate-specific heterozygous *Pten* mutations with various *Tgfbr2* genotypes supports the idea that loss of *Pten* is the tumor initiating event. This is further supported by the fact that mice with homozygous *Tgfbr2* deletion in the prostate and wild type *Pten* are normal out to at least 70 weeks. Although tumors arise in the *Pten* heterozygous prostates over a relatively long time-course, this is consistent with the acquisition of a second mutation that occurs with relatively low frequency, such as inactivation of the other allele of *Pten*. This has been suggested to be a major route by which *Pten* heterozygous mutations in mouse prostate can become tumorigenic [36]. All *Pten* heterozygous tumors analyzed, irrespective of the *Tgfbr2* genotype, had high levels of phospho-Akt, specifically in the phenotypic regions of the prostate. In contrast, all *Pten* heterozygous prostates in which no phenotype was apparent lacked significant phospho-Akt signal. Thus it is likely that in this context Akt signaling and any other pathways downstream of Pten have been activated by loss of the additional *Pten* allele. One interesting possibility raised by the low frequency and slow onset of invasive cancer in *Tg-AKT;Tgfbr2*$^{r/r}$ mice is that this occurs following the acquisition of some other genetic change, that in combination with AKT activation and inactivation of the TGFβ pathway, allows for rapid progression to invasive cancer.

We observed a high frequency of metastasis to the local lymph nodes and lungs in animals with reduced TGFβ signaling. Given the known pro-metastatic functions of TGFβ signaling this might be somewhat surprising, although similar increases in metastasis in the *Pten;Smad4* double null model have also been reported [30]. In this context it is interesting to note that all of the *Pten* null mice with heterozygous *Tgfbr2* mutations had lymph node metastases, whereas only two thirds of *Pten*$^{r/r}$*;Tgfbr2*$^{r/r}$ mice did. Additionally, we identified lung metastases in all four *Pten*$^{r/r}$*;Tgfbr2*$^{+/r}$ mice examined, consistent with the idea that partial inactivation of TGFβ signaling might allow for both increased proliferation and increased metastasis. However, an alternative possibility is that more metastases were found in *Pten*$^{r/r}$*;Tgfbr2*$^{+/r}$ mice simply because they survived longer than double nulls.

Conditional *Smad4* mutation, in the background of a prostate-specific *Pten* null allele results in prostate tumors in mice, which have a median survival time of less than 23 weeks [30]. Our analysis of *Pten*$^{r/r}$*;Tgfbr2*$^{r/r}$ mice demonstrates the presence of micro-invasive cancer by as

early as 8 weeks of age, and have a median survival time of less than 13 weeks, suggesting that loss of the Tgfbr2 results in a much more rapid acceleration of tumor progression than with loss of Smad4. This is consistent with the fact that other Smad-independent pathways can be activated downstream of the TGFβ receptors [37, 38]. Additionally, it is possible that some Smad-dependent transcriptional activity is present even in the absence of Smad4. However, it should be noted that while both analyses were carried out in similar mixed strain backgrounds, it is possible that strain differences may contribute to the difference in phenotypes. TGFβ signaling can be both anti-proliferative and pro-metastatic, making its role in tumor progression somewhat complex [21, 22]. Therefore, it will be of interest to further dissect how TGFβ signaling and the Smads restrain the progression from HGPIN to invasive cancer, and yet promote metastatic disease.

In summary, we have shown that TGFβ signaling is induced in the prostate by Pten loss, or by activation of Akt, and functions to keep in check the tumorigenic effects of Pten/Akt pathway activation. This work, together with that analyzing *Smad4* and *Pten* mutations [30], clearly places TGFβ signaling as a key regulator of prostate cancer progression.

Materials and Methods

Mice

All animal procedures were approved by the Animal Care and Use Committee of the University of Virginia, which is fully accredited by the AAALAC. Conditional alleles of *Tgfbr2* and *Pten* [10, 31] were combined with the *Pb-Cre4* transgene to drive prostate epithelium-specific deletion [32]. The prostate-specific *caAKT1* transgene [16] was obtained from the NCI MMHCC Repository. Experimental animals were analyzed on a mixed C57BL/6 x FVB background. To combine the alleles, $Tgfbr2^{f/f}$ and *PbCre4* mice on a C57BL/6 background were crossed to FVB $Pten^{f/f}$ mice. These offspring were then intercrossed to generate the cohorts from which experimental animals were generated. *Tg-Akt* (FVB) were crossed with *PbCre4* and $Tgfbr2^{f/f}$ (C57BL/6) and the experimental animals generated from intercrossing the offspring. Given the lower penetrance of the *Tg-Akt* phenotype, the majority of *Tg-Akt* mice with wild type *Tgfbr2* analyzed, were $Tg\text{-}Akt^{+};Tgfbr2^{f/f};Cre^{-}$ littermates of $Akt^{+};Tgfbr2^{r/r}$ mice ($Akt^{+};Tgfbr2^{f/f\,f};Cre^{+}$). Significance testing for Kaplan Meier curves was performed using a log rank test (http://bioinf.wehi.edu.au/software/russell/logrank/).

DNA and RNA analyses

Genomic DNA for genotype analysis was purified from ear punch (at P21) by HotShot [39], and genotypes were determined by PCR. RNA was isolated and purified using Absolutely RNA kit (Stratagene). cDNA was generated using Superscript III (Invitrogen), and analyzed in triplicate by real time PCR using a BioRad MyIQ cycler and Sensimix Plus SYBRgreen plus FITC mix (Quantace), with intron spanning primer pairs, selected using Primer3 (http://frodo.wi.mit.edu/). Expression was normalized to Rpl4 and cyclophilin using the delta Ct method.

Histology, IHC and IF

Immunohistochemistry (IHC) and immunofluorescence (IF) analyses were performed as previously described [40-42]. Whole prostate images were taken with a Leica MZ16 stereomicroscope and QImaging 5.0 RTV digital camera. IF images were captured on an Olympus BX51 microscope and DP70 digital camera, or Zeiss AxioObserver and manipulated in Volocity and Adobe Photoshop. For analysis of N:C ratios of pSmad2, at least 40 cells from multiple ducts were chosen based on the DAPI image, and the mean fluorescence intensity in a fixed area of the nucleus and cytoplasm was determined using Image J. At least 2 animals of each genotype were analyzed an representative data from multiple individual animals is shown. Antibodies for IF and IHC were against: phospho-Smad2 (Millipore AB3849), Smad4 (Millipore 04-1033), Tgfbr2 (Novus NBP1-19434), phospho-Akt (Cell Signaling 9277), Cyclin D (Santa Cruz sc-753), p27 (BD Transduction Labs 610242), Ki-67 and (DakoCytomation M7249).

Western blotting

Proteins were separated by SDS-PAGE, transferred to Immobilon-P (Millipore) and proteins were visualized using SuperSignal West Pico ECL (Pierce). Primary antibodies were against phospho-Smad2 (Millipore AB3849), Smad4 (Millipore 04-1033), Tgfbr2 (Santa Cruz sc-400) and γ-tubulin (Sigma T6557).

Acknowledgements

We thank Sharon Birdsall and Marya Brown for technical assistance, Doug DeSimone for use of the Zeiss microscope, Anindya Dutta and Dan Gioeli for helpful discussions and Tiffany Melhuish for expert advice and assistance. This work was supported by a Program Project Grant from the National Cancer Institute (2P01CA104106 to B. Paschal and D. Wotton), and by a pilot grant from the UVA Cancer Center (funded from the CCSG P30 CA44579, the James and Rebecca Craig Foundation, and UVA Women's Oncology fund) to D. Wotton.

References

1. Cairns P, Okami K, Halachmi S, Halachmi N, Esteller M, Herman JG, et al. Frequent inactivation of PTEN/MMAC1 in primary prostate cancer. Cancer Res. 1997; 57(22):4997–5000. [PubMed: 9371490]
2. Dahia PL. PTEN, a unique tumor suppressor gene. Endocrine-related cancer. 2000; 7(2):115–29. [PubMed: 10903528]
3. Suzuki H, Freije D, Nusskern DR, Okami K, Cairns P, Sidransky D, et al. Interfocal heterogeneity of PTEN/MMAC1 gene alterations in multiple metastatic prostate cancer tissues. Cancer Res. 1998; 58(2):204–9. [PubMed: 9443392]
4. Wang SI, Parsons R, Ittmann M. Homozygous deletion of the PTEN tumor suppressor gene in a subset of prostate adenocarcinomas. Clin Cancer Res. 1998; 4(3):811–5. [PubMed: 9533551]
5. Di Cristofano A, Pandolfi PP. The multiple roles of PTEN in tumor suppression. Cell. 2000; 100(4): 387–90. [PubMed: 10693755]
6. Yamada KM, Araki M. Tumor suppressor PTEN: modulator of cell signaling, growth, migration and apoptosis. Journal of cell science. 2001; 114(Pt 13):2375–82. [PubMed: 11559746]
7. Podsypanina K, Ellenson LH, Nemes A, Gu J, Tamura M, Yamada KM, et al. Mutation of Pten/Mmac1 in mice causes neoplasia in multiple organ systems. Proc Natl Acad Sci U S A. 1999; 96(4): 1563–8. [PubMed: 9990064]
8. Di Cristofano A, Pesce B, Cordon-Cardo C, Pandolfi PP. Pten is essential for embryonic development and tumour suppression. Nat Genet. 1998; 19(4):348–55. [PubMed: 9697695]

9. Ma X, Ziel-van der Made AC, Autar B, van der Korput HA, Vermeij M, van Duijn P, et al. Targeted biallelic inactivation of Pten in the mouse prostate leads to prostate cancer accompanied by increased epithelial cell proliferation but not by reduced apoptosis. Cancer Res. 2005; 65(13):5730–9. [PubMed: 15994948]
10. Suzuki A, Yamaguchi MT, Ohteki T, Sasaki T, Kaisho T, Kimura Y, et al. T cell-specific loss of Pten leads to defects in central and peripheral tolerance. Immunity. 2001; 14(5):523–34. [PubMed: 11371355]
11. Trotman LC, Niki M, Dotan ZA, Koutcher JA, Di Cristofano A, Xiao A, et al. Pten dose dictates cancer progression in the prostate. PLoS biology. 2003; 1(3):E59. [PubMed: 14691534]
12. Wang S, Gao J, Lei Q, Rozengurt N, Pritchard C, Jiao J, et al. Prostate-specific deletion of the murine Pten tumor suppressor gene leads to metastatic prostate cancer. Cancer cell. 2003; 4(3): 209–21. [PubMed: 14522255]
13. Bayascas JR, Leslie NR, Parsons R, Fleming S, Alessi DR. Hypomorphic mutation of PDK1 suppresses tumorigenesis in PTEN(+/−) mice. Curr Biol. 2005; 15(20):1839–46. [PubMed: 16243031]
14. Chen ML, Xu PZ, Peng XD, Chen WS, Guzman G, Yang X, et al. The deficiency of Akt1 is sufficient to suppress tumor development in Pten+/− mice. Genes Dev. 2006; 20(12):1569–74. [PubMed: 16778075]
15. Majumder PK, Febbo PG, Bikoff R, Berger R, Xue Q, McMahon LM, et al. mTOR inhibition reverses Akt-dependent prostate intraepithelial neoplasia through regulation of apoptotic and HIF-1-dependent pathways. Nature medicine. 2004; 10(6):594–601.
16. Majumder PK, Yeh JJ, George DJ, Febbo PG, Kum J, Xue Q, et al. Prostate intraepithelial neoplasia induced by prostate restricted Akt activation: the MPAKT model. Proc Natl Acad Sci U S A. 2003; 100(13):7841–6. [PubMed: 12799464]
17. Heldin C-H, Miyazono K, ten Dijke P. TGF-ß signalling from cell membrane to nucleus through SMAD proteins. Nature. 1997; 390:465–71. [PubMed: 9393997]
18. Massagué J. TGFß signal transduction. Annu Rev Biochem. 1998; 67:753–91. [PubMed: 9759503]
19. Zhang Y, Derynck R. Regulation of Smad signaling by protein associations and signaling crosstalk. Trends in Cell BIology. 1999; 9:274–9. [PubMed: 10370243]
20. Massague J, Seoane J, Wotton D. Smad transcription factors. Genes Dev. 2005; 19(23):2783–810. [PubMed: 16322555]
21. Ikushima H, Miyazono K. TGFbeta signalling: a complex web in cancer progression. Nat Rev Cancer. 2010; 10(6):415–24. [PubMed: 20495575]
22. Massague J, Blain SW, Lo RS. TGFbeta signaling in growth control, cancer, and heritable disorders. Cell. 2000; 103(2):295–309. [PubMed: 11057902]
23. Levy L, Hill CS. Alterations in components of the TGF-beta superfamily signaling pathways in human cancer. Cytokine & growth factor reviews. 2006; 17(1-2):41–58. [PubMed: 16310402]
24. Aitchison AA, Veerakumarasivam A, Vias M, Kumar R, Hamdy FC, Neal DE, et al. Promoter methylation correlates with reduced Smad4 expression in advanced prostate cancer. The Prostate. 2008; 68(6):661–74. [PubMed: 18213629]
25. Zhao H, Shiina H, Greene KL, Li LC, Tanaka Y, Kishi H, et al. CpG methylation at promoter site -140 inactivates TGFbeta2 receptor gene in prostate cancer. Cancer. 2005; 104(1):44–52. [PubMed: 15895377]
26. Guo Y, Jacobs SC, Kyprianou N. Down-regulation of protein and mRNA expression for transforming growth factor-beta (TGF-beta1) type I and type II receptors in human prostate cancer. Int J Cancer. 1997; 71(4):573–9. [PubMed: 9178810]
27. Kim IY, Ahn HJ, Zelner DJ, Shaw JW, Lang S, Kato M, et al. Loss of expression of transforming growth factor beta type I and type II receptors correlates with tumor grade in human prostate cancer tissues. Clin Cancer Res. 1996; 2(8):1255–61. [PubMed: 9816295]
28. Williams RH, Stapleton AM, Yang G, Truong LD, Rogers E, Timme TL, et al. Reduced levels of transforming growth factor beta receptor type II in human prostate cancer: an immunohistochemical study. Clin Cancer Res. 1996; 2(4):635–40. [PubMed: 9816213]

29. Ding Z, Wu CJ, Chu GC, Xiao Y, Ho D, Zhang J, et al. SMAD4-dependent barrier constrains prostate cancer growth and metastatic progression. Nature. 2011; 470(7333):269–73. [PubMed: 21289624]

30. Ding Z, Wu CJ, Jaskelioff M, Ivanova E, Kost-Alimova M, Protopopov A, et al. Telomerase reactivation following telomere dysfunction yields murine prostate tumors with bone metastases. Cell. 2012; 148(5):896–907. [PubMed: 22341455]

31. Chytil A, Magnuson MA, Wright CV, Moses HL. Conditional inactivation of the TGF-beta type II receptor using Cre:Lox. Genesis. 2002; 32(2):73–5. [PubMed: 11857781]

32. Wu X, Wu J, Huang J, Powell WC, Zhang J, Matusik RJ, et al. Generation of a prostate epithelial cell-specific Cre transgenic mouse model for tissue-specific gene ablation. Mech Dev. 2001; 101(1-2):61–9. [PubMed: 11231059]

33. Debes JD, Tindall DJ. Mechanisms of androgen-refractory prostate cancer. N Engl J Med. 2004; 351(15):1488–90. [PubMed: 15470210]

34. Majumder PK, Grisanzio C, O'Connell F, Barry M, Brito JM, Xu Q, et al. A prostatic intraepithelial neoplasia-dependent p27 Kip1 checkpoint induces senescence and inhibits cell proliferation and cancer progression. Cancer cell. 2008; 14(2):146–55. [PubMed: 18691549]

35. Di Cristofano A, De Acetis M, Koff A, Cordon-Cardo C, Pandolfi PP. Pten and p27KIP1 cooperate in prostate cancer tumor suppression in the mouse. Nat Genet. 2001; 27(2):222–4. [PubMed: 11175795]

36. Kim J, Roh M, Doubinskaia I, Algarroba GN, Eltoum IE, Abdulkadir SA. A mouse model of heterogeneous, c-MYC-initiated prostate cancer with loss of Pten and p53. Oncogene. 2012; 31(3): 322–32. [PubMed: 21685943]

37. Sorrentino A, Thakur N, Grimsby S, Marcusson A, von Bulow V, Schuster N, et al. The type I TGF-beta receptor engages TRAF6 to activate TAK1 in a receptor kinase- independent manner. Nat Cell Biol. 2008; 10(10):1199–207. [PubMed: 18758450]

38. Yamaguchi K, Shirakabe K, Shibuya H, Irie K, Oishi I, Ueno N, et al. Identification of a member of the MAPKKK family as a potential mediator of TGF-beta signal transduction. Science. 1995; 270:2008–11. [PubMed: 8533096]

39. Truett GE, Heeger P, Mynatt RL, Truett AA, Walker JA, Warman ML. Preparation of PCR-quality mouse genomic DNA with hot sodium hydroxide and tris (HotSHOT). Biotechniques. 2000; 29(1):52, 4. [PubMed: 10907076]

40. Bartholin L, Melhuish TA, Powers SE, Goddard-Leon S, Treilleux I, Sutherland AE, et al. Maternal Tgif is required for vascularization of the embryonic placenta. Dev Biol. 2008; 319(2): 285–97. [PubMed: 18508043]

41. Galgano MT, Conaway M, Spencer AM, Paschal BM, Frierson HF Jr. PRK1 distribution in normal tissues and carcinomas: overexpression and activation in ovarian serous carcinoma. Human pathology. 2009; 40(10):1434–40. [PubMed: 19427017]

42. Powers SE, Taniguchi K, Yen W, Melhuish TA, Shen J, Walsh CA, et al. Tgif1 and Tgif2 regulate Nodal signaling and are required for gastrulation. Development. 2010; 137(2):249–59. [PubMed: 20040491]

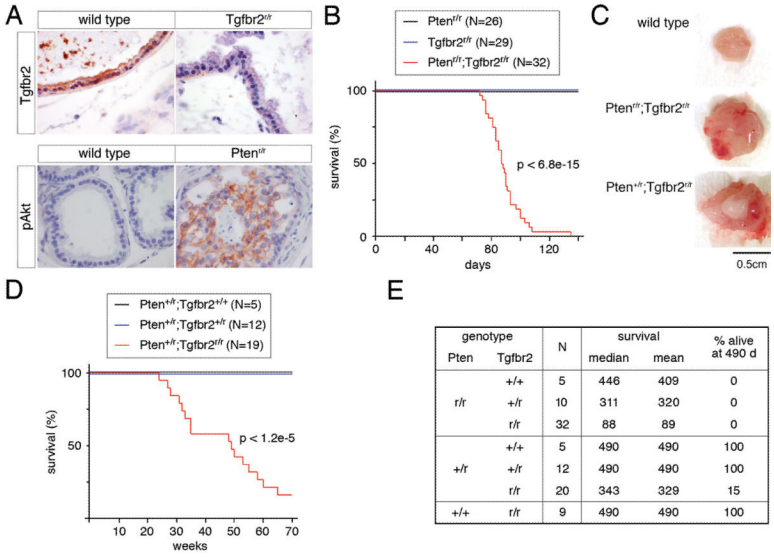

genotype Pten	genotype Tgfbr2	N	survival median	survival mean	% alive at 490 d
	+/+	5	446	409	0
r/r	+/r	10	311	320	0
	r/r	32	88	89	0
	+/+	5	490	490	100
+/r	+/r	12	490	490	100
	r/r	20	343	329	15
+/+	r/r	9	490	490	100

Figure 1. Early onset of prostate cancer in mice with deletion of *Pten* and *Tgfbr2*

A) Prostates of the indicated genotypes ($Tgfbr2^{r/r}$ and $Pten^{r/r}$ indicate prostate specific deletion of *Tgfbr2* and *Pten*) were analyzed by IHC for Tgfbr2 and Akt phosphorylated on serine 473 (pAkt). B) Kaplan-Meier plots for mice with homozygous deletion of *Pten*, *Tgfbr2* or both genes in the prostate are shown. The p-value (log-rank test) for comparison of $Pten^{r/r};Tgfbr2^{r/r}$ with $Pten^{r/r}$ is shown. C) Examples of whole prostates from the indicated genotypes are shown. The $Pten^{r/r};Tgfbr2^{r/r}$ was euthanized at 88 days and the $Pten^{+/r};Tgfbr2^{r/r}$ at 212 days, due to tumor burden. D) Kaplan-Meier plots for mice with prostate specific heterozygous *Pten* mutations and the indicated *Tgfbr2* genotypes are shown. The p-value is for comparison of $Pten^{+/r};Tgfbr2^{r/r}$ with $Pten^{+/r};Tgfbr2^{+/r}$. E) A summary of the tumor-free survival data for animals of the indicated genotypes is shown. Genotypes refer to prostate specific mutations of the indicated genes. Only mice that were carried out to 70 weeks (490 days) or that were euthanized due to tumor burden are included in this analysis.

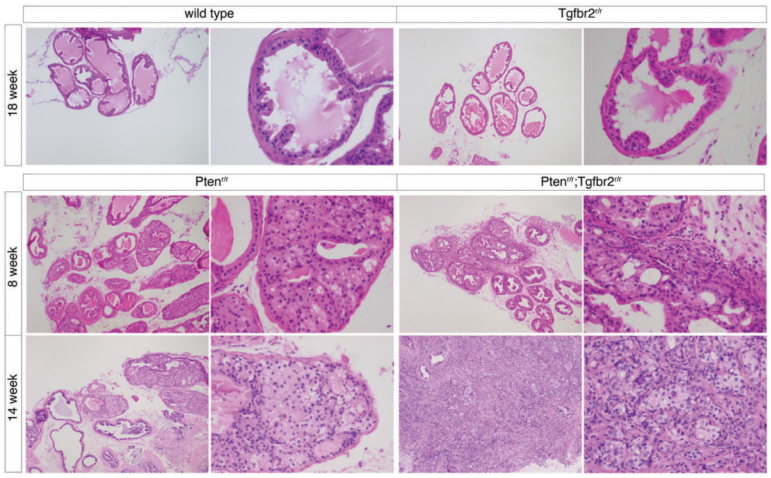

Figure 2. Invasive cancer in the double null prostate

Hematoxylin and eosin (H&E) stained sections of prostates from mice of the indicated genotypes and ages are shown.

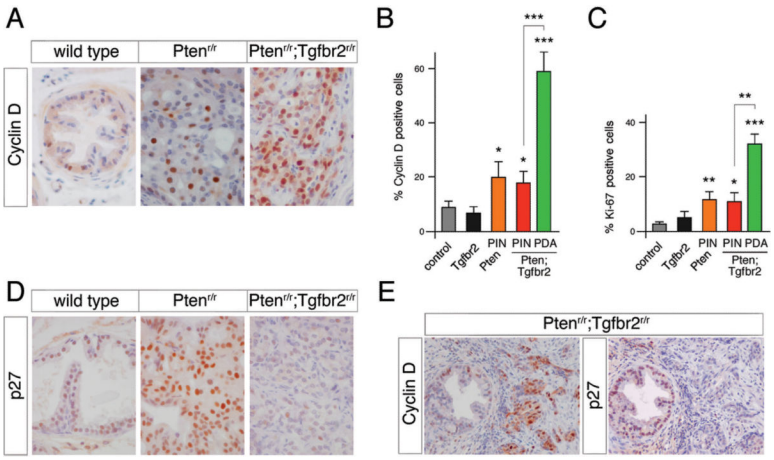

Figure 3. Analysis of proliferation in mutant prostate

A) Prostates of the indicated genotypes were analyzed by IHC for cyclin D. Prostates from three mice of each genotype were analyzed for cyclin D (B) or Ki-67 (C) by IHC. The percentage of positive cells (mean + s.d.) is plotted for each genotype. HGPIN and invasive cancer (PDA; poorly differentiated adenocarcinoma) in the double mutant were counted separately. Significance (by Student's T test) is shown for comparison to the wild type (control) and for comparison between HGPIN and PDA in the double mutants. * : $p < 0.05$, ** : $p < 0.01$, *** : $p < 0.001$. (D) Expression of the p27 CDK inhibitor was analyzed by IHC in the indicated genotypes. (E) Serial sections of a *Pten*$^{r/r}$*;Tgfbr2*$^{r/r}$ prostate, in which both invasive cancer and a more normal duct are visible, were analyzed for Cyclin D and p27.

A

genotype Pten	genotype Tgfbr2	Total	LN mets N	LN mets %
	+/+	6	1	16.7
r/r	+/r	9	9	100
	r/r	35	23	65.7
+/r	r/r	11	4	36.4
castrated				
r/r	r/r	14	5	35.7

D

genotype Pten	genotype Tgfbr2	Total	Lung mets N	Lung mets %
r/r	+/r	4	4	100
	r/r	11	6	54.5

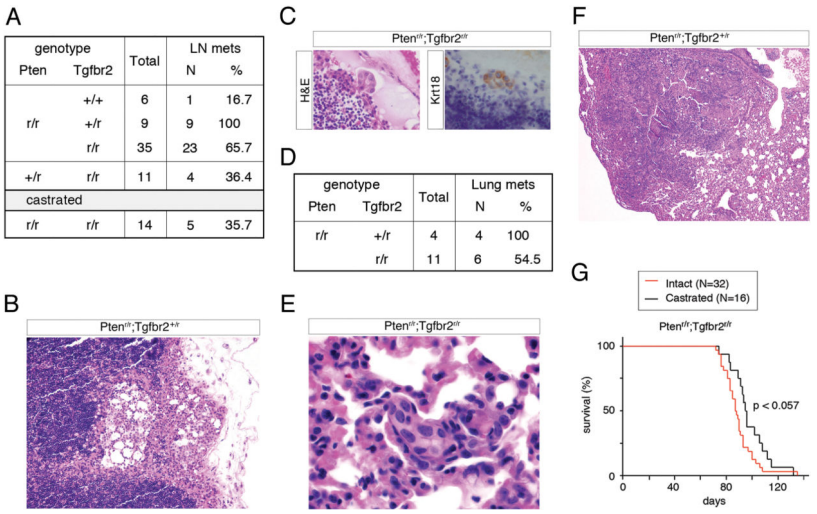

Figure 4. Analysis of metastasis and castration resistance

A) The number of animals analyzed and the number of lymph node metastases found are shown, together with the percentage of animals with metastases. The number of lymph node metastases found in *Pten*$^{r/r}$*;Tgfbr2*$^{r/r}$ mice that had been castrated at either 6 weeks or 9-11 weeks of age is also shown. B) A lymph node metastasis from a *Pten*$^{r/r}$*;Tgfbr2*$^{+/r}$ mouse (49 weeks old) is shown stained with H&E. C) An example of a lymph node micro-metastasis from a *Pten*$^{r/r}$*;Tgfbr2*$^{r/r}$ (88 days old) is shown, stained with H&E and for keratin 18 by IHC. D) The frequency of lung metastases in *Pten*$^{r/r}$*;Tgfbr2*$^{r/r}$ and *Pten*$^{r/r}$*;Tgfbr2*$^{+/r}$ mice is shown. H&E images of lung metastases are shown from an 83 day old *Pten*$^{r/r}$*;Tgfbr2*$^{r/r}$ mouse (E) and a 54 week *Pten*$^{r/r}$*;Tgfbr2*$^{+/r}$ mouse (F). G) Kaplan-Meier plots comparing survival of *Pten*$^{r/r}$*;Tgfbr2*$^{r/r}$ with mice of the same genotype that were castrated at 6-11 weeks of age.

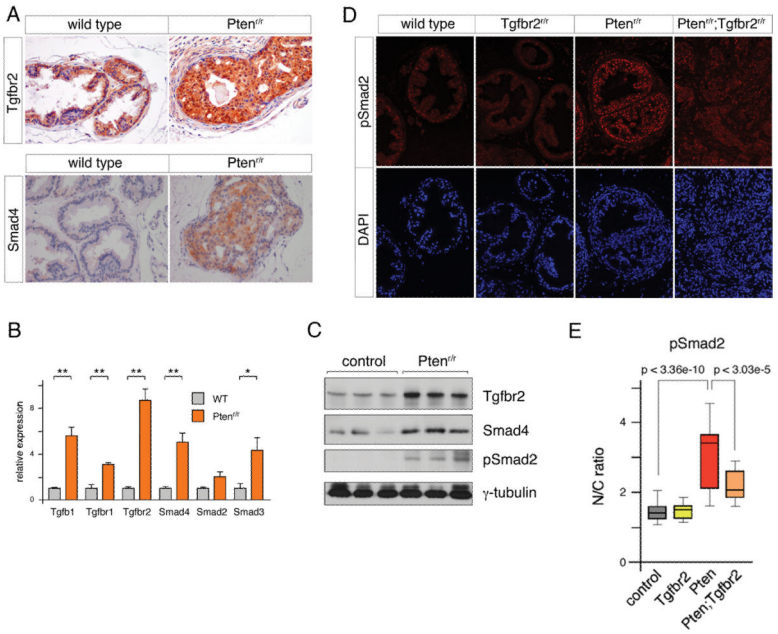

Figure 5. Expression of TGFβ pathway components in *Pten* null prostates

A) Expression of Tgfbr2 and Smad4 was analyzed by IHC in control and *Pten* null prostate. B) Expression of a panel of genes encoding mediators of the TGFβ pathway was analyzed by qRT-PCR in wild type or *Pten* null prostate. Relative expression is shown (arbitrary units, mean + s.d.) from three animals per genotype. p-values were determined by Student's T test. ** : $p < 0.05$, ** : $p < 0.01$. C) Expression of Smad4, Tgfbr2 and pSmad2 was analyzed by western blot in prostates from control and *Pten* null mice. D) Prostates were analyzed by IF for Smad2 phosphorylated at its carboxyl-terminus (pSmad2) as an indicator of Smad activation. Coincident DAPI staining is shown below. E) At least 40 cells each (selected based on DAPI stain) were analyzed for the mean nuclear to cytoplasmic ratio of the pSmad2 signal. Data are shown as box plots (median, 5th, 25th, 75th and 95th percentiles), with the p-values (determined by Student's T test) for comparison of *Pten* null to control and *Pten* null to double null.

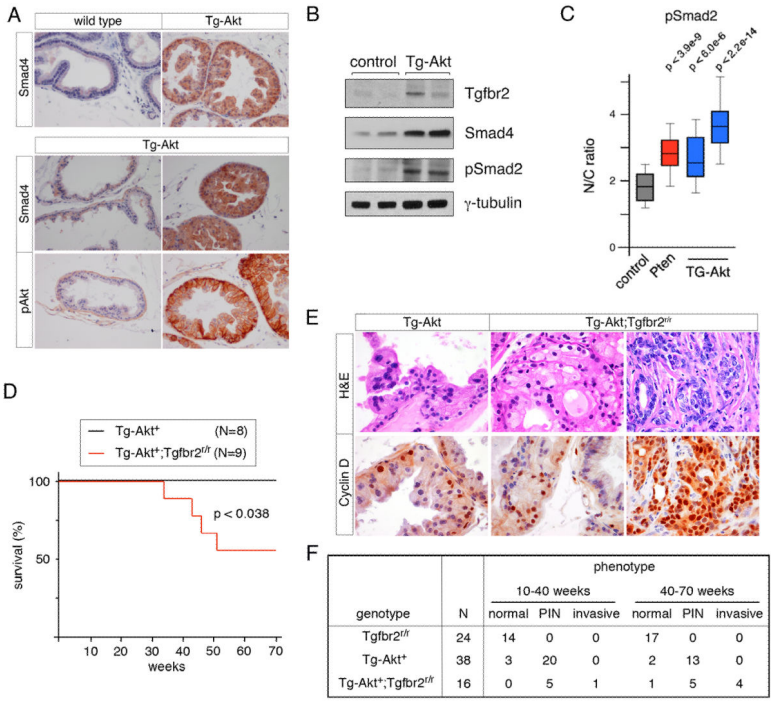

genotype	N	phenotype					
		10-40 weeks			40-70 weeks		
		normal	PIN	invasive	normal	PIN	invasive
$Tgfbr2^{f/f}$	24	14	0	0	17	0	0
$Tg\text{-}Akt^{+}$	38	3	20	0	2	13	0
$Tg\text{-}Akt^{+};Tgfbr2^{f/f}$	16	0	5	1	1	5	4

Figure 6. Induction of TGFβ signaling downstream of AKT activation

A) Prostates from control and *TG-AKT1* mice were analyzed for Smad4 and for pAkt by IHC. B) Control and *TG-AKT1* ventral prostates were analyzed by western blot for Smad4, Tgfbr2 and pSmad2. C) The nuclear to cytoplasmic ratio of pSmad2 mean fluorescence intensity was analyzed in at least 40 cells each in two pAkt-positive *TGAKT1* prostates and from control and *Pten* null prostates for comparison. Data are shown as box plots (median, 5^{th}, 25^{th}, 75^{th} and 95^{th} percentiles). p-values (determined by Student's T test) for comparison of *Pten* null and *TG-AKT1* prostates to the control are shown. D) Kaplan-Meier plots comparing survival of *TG-AKT1* mice with *TG-AKT1* mice that were null for the *Tgfbr2* gene are shown. E) *TG-AKT1* and *TG-AKT1;Tgfbr2*$^{r/r}$ ventral prostates were stained with H&E and for cyclin D, by IHC. Two examples of *TGAKT1;Tgfbr2*$^{r/r}$ prostates are shown: One (right) shows invasive cancer, the other (left) has only HGPIN and is indistinguishable from the *TG-AKT1*. F) The phenotypes of animals euthanized between 10 and 70 weeks of age are summarized. Ventral prostates were examined by H&E and were scored as either normal, PIN (both focal and extensive HGPIN) or invasive cancer.